

THE EFFECT OF MICROSTRUCTURE ON FRACTURE OF A NEW HIGH TOUGHNESS TITANIUM ALLOY

J. C. Chesnutt*, C. G. Rhodes*, R. G. Berryman**,
F. H. Froes*** and J. C. Williams****

INTRODUCTION

The design requirements for current and near-future high performance, lightweight aircraft has emphasized the need for titanium alloys with strength-toughness combinations exceeding those presently available in alloys such as Ti-6Al-4V. This paper briefly describes the development of such an alloy and discusses methods of controlling the fracture properties of the alloy through manipulation of microstructure by thermomechanical processing and heat treatment.

The alloy, Ti-4.5Al-5Mo-1.5Cr (CORONA-5), was developed under Naval Air Systems Command sponsorship [1,2] to meet a fracture toughness goal of $110 \text{ MPa}\cdot\text{m}^{1/2}$ at a minimum ultimate tensile strength of 930 MPa. During the first year of the program, studies were conducted to select the alloy composition, and during the second year the effect of processing on microstructure and fracture properties was investigated. Results of this study showed that fracture properties could be significantly affected by microstructural features such as α -phase along prior β grain boundaries and by α -phase size, distribution and morphology. The remainder of this paper will describe some of the microstructures achieved by using various thermomechanical processing sequences and the effect of these microstructures on fracture properties.

RESULTS

The results will be divided into two sections. The first describes the variations of microstructure and the second describes the effect of microstructure on fracture toughness and fracture topography.

Microstructure

CORONA-5 is a two phase, $\alpha + \beta$ titanium alloy which exhibits a duplex microstructure. The microstructure consists of relatively coarse primary α and finer precipitated α . The volume fraction, size and morphology of the primary α is dependent on prior forging history, whereas the spacing and volume fraction of the precipitated α depends largely on the post-forging heat treatment. The morphology and distribution of the primary α appears to influence the fracture path to a predominant degree while the precipitated α largely controls the strength of the alloy. Examples of these two microstructural variables will be illustrated below.

*Rockwell International, Science Center, Thousand Oaks, CA.

**Rockwell International, Los Angeles Aircraft Division, El Segundo, CA.

***Colt Industries, Crucible Materials Research Center, Pittsburgh, PA.

****Department of Metallurgy and Materials Science, Carnegie-Mellon University, Pittsburgh, PA.

The range of primary α morphologies and distributions which can be achieved in CORONA-5 by varying the forging finishing temperatures are shown in Figures 1(a)-(c). Figure 1(a) shows the microstructure from forging at temperatures above the β -transus (hereafter referred to as β -forged). This microstructure consists of coarse, acicular primary α -plates with an extensive network of α -phase along the prior β grain boundaries. Since the acicular α forms in this case by nucleation and growth during cooling, the plates have a high aspect ratio.

Figure 1(b) shows the microstructure which results from finish forging at a temperature high in the α/β phase field (hereafter referred to as high α/β -forged). This microstructure consists of primary α which has an acicular morphology, but with a smaller aspect ratio than in the β -forged material. The microstructure also exhibits some grain boundary α , but it is not as pronounced or as continuous as in the β -forged material. Figure 1(c) shows the microstructure which results from finish forging at temperatures lower in the α/β phase field (hereafter referred to as low α/β -forged). This microstructure, with no detectable remnants of α precipitation at the prior β grain boundaries, consists of slightly elongated primary α particles which are uniformly distributed. The details of the forging operations used to produce these microstructures have been described in reference [3] where the three conditions are identified as forging 1, 3 and 11 respectively.

Post forging heat treatment controls the α precipitation process as shown in Figures 2(a)-(c). There were two heat treatments used for the microstructures described here. These were both duplex annealing treatments, the details of which are included in Table I. The effect of these final heat treatments can be seen by examining Table I and comparing the properties of the material which was given the high final treatment with those of the material given the low final treatment. The high final treatment produced higher toughness at the expense of strength when compared to the low final treatment. These variations in strength result from variations of α -phase precipitate size and spacing within the retained β matrix. Comparison of Figure 2(a) with Figure 2(b) and 2(c) reveals that the high final heat treatment resulted in larger α particles with larger spacings compared to the low final treatment. The effect of final heat treatment is comparable for forgings finished either above or below the β transus since the first anneal of the duplex annealing cycle always controls the β phase composition prior to precipitation during the second anneal.

Fracture Properties and Fractography

The effects of thermo-mechanical processing on fracture toughness can be seen by comparing the fracture toughness values shown in Table I for the three forging conditions in the same high final heat treatment condition. These data show that the β -forged material is the toughest. Scanning electron fractography has been used to help explain this observation. Analysis of the scanning electron fractographs in Figure 3 reveals that fracture toughness can be directly related to fracture path and to the path-controlling microstructure.

The fracture surface of the β -forged specimen shown in Figure 3 is highly irregular; this results from extensive crack branching and secondary cracking which occurs on the scale of the prior β grain size. This type of tortuous crack path increases the net area of the crack plane and would thereby be expected to increase the toughness of the material. This observation is consistent with the effect of β processing on the toughness

of other high strength titanium alloys, such as Ti-6Al-2Sn-4Zr-6Mo [4]. A tortuous fracture path which is caused by microstructural features of a different scale is achieved in the high α/β -forged material, Figure 3(b). This path results from the high aspect ratio of the primary α , Figure 1(b). The elongated α particles provide preferential crack paths either along the major axis of the particle or at the interface between the particle and the β matrix. In addition, remnant grain boundary α may provide a preferential path as it does in the β -forged material. These preferential crack paths lead to crack branching and to secondary cracking similar to that in the β -forged material, but on a finer scale, cf Figure 3(b) and 3(a). Comparing the data for the low α/β -forged material with that of the high α/β -forged material, indicates that as the primary α particle aspect ratio is reduced, the fracture toughness decreases significantly. This decrease in fracture toughness is accompanied by a fracture which is characterized by a flat, smooth fracture face comprised of small, equiaxed dimples, Figure 3(c). In titanium alloys, this type of fracture is often associated with low toughness/high strength conditions, especially in higher strength alloys [4].

Since either prior β grain boundaries or high aspect ratio primary α provide a more tortuous fracture path and thereby enhance toughness to a similar degree, considerable latitude is available for microstructural control of fracture properties. This would permit use of an α/β -processed condition with high aspect ratio primary α in those situations in which a β -processed microstructure might degrade other significant properties. Finally, it should be noted that several of the ultimate tensile strengths reported in Table I are 2-3% below the goal value; experience from the previous work [2] has shown that minor adjustments of the final heat treatment will permit achievement of goal strength at toughnesses in excess of goal toughness.

CONCLUSIONS

It has been shown that the microstructure of CORONA-5 forgings can be significantly altered by thermo-mechanical processing and heat treatment, and that the microstructures produced affect fracture properties. Specifically, finish forging above the beta transus results in a coarse Widmanstätten α structure, while finishing below the beta transus results in a primary α aspect ratio directly related to the temperature (below the beta transus) to which the alloy is exposed; i.e., the higher the forging temperature (either blocking or finishing), the greater will be the primary α aspect ratio. The microstructures that were developed affect the fracture toughness of these forgings on three distinct scales:

- 1) Large, equiaxed prior β grains of the β -processed conditions promote crack branching and enhance toughness.
- 2) Primary α particles with large aspect ratios provide more tortuous crack paths with an attendant toughness increase, while equiaxed primary α provides a lower energy fracture path, since the fracture can propagate in an almost planar manner.
- 3) The α phase precipitated in the retained β during final anneal and aging can promote strength at the expense of toughness (fine α from a low temperature anneal and age) or toughness at the expense of strength (coarse α from a high temperature anneal and age). The effect probably results from a localized effect of the precipitate on yield strength and thereby toughness.

In summary, manipulation of processing parameters to produce β or α/β structures, to affect primary α aspect ratios, and to affect α precipitation in the retained β provides strong methods for tailoring toughness and strength properties in CORONA-5.

ACKNOWLEDGMENT

This work was sponsored by the Naval Air Systems Command under Contracts N00019-74-C-0273 and N00019-75-C-0208.

REFERENCES

1. BERRYMAN, R. G., WILLIAMS, J. C., CHESNUTT, J. C., RHODES, C. G., FROES, F. H. and MALONE, R. F., Final Engineering Report, Naval Air Systems Command Contract No. N00019-73-C-0335, "High Toughness Titanium Alloy Development", July 1974, TFD-74-657.
2. BERRYMAN, R. G., FROES, F. H., CHESNUTT, J. C., WILLIAMS, J. C. and MALONE, R. F., Final Engineering Report, Naval Air Systems Command Contract No. N00019-74-C-0273, "High Toughness of Titanium Alloys", July 1975, TFD-75-640.
3. BERRYMAN, R. G., CHESNUTT, J. C., FROES, F. H. and RHODES, C. G., Final Engineering Report, Naval Air Systems Command Contract No. N00019-75-C-0208, "High Toughness Titanium Alloy Development", June 1976, TFD-76-471.
4. CHESNUTT, J. C., RHODES, C. G. and WILLIAMS, J. C., in Fractography-Microscopic Cracking Processes, ASTM STP 600, American Society for Testing and Materials, Philadelphia, 1975, pp.99-138.

Table 1 Mechanical Properties of CORONA-5

Forging No.	Microstructural Condition	Final Heat Treatment	0.2% Offset Yield Stress MPa	Ultimate Tensile Strength MPa	Fracture Toughness $\text{MPa}\cdot\text{m}^{1/2}$
1	β Forged	High ¹	810	911	151
2	β Forged	Low ²	891	991	112
3	High α/β Forged	High ¹	828	903	144
11	Low α/β Forged	High ¹	846	906	109

1. 843°C/8 hr + air cool + 704°C/4 hr + air cool
2. 802°C/16 hr + air cool + 607°C/4 hr + air cool

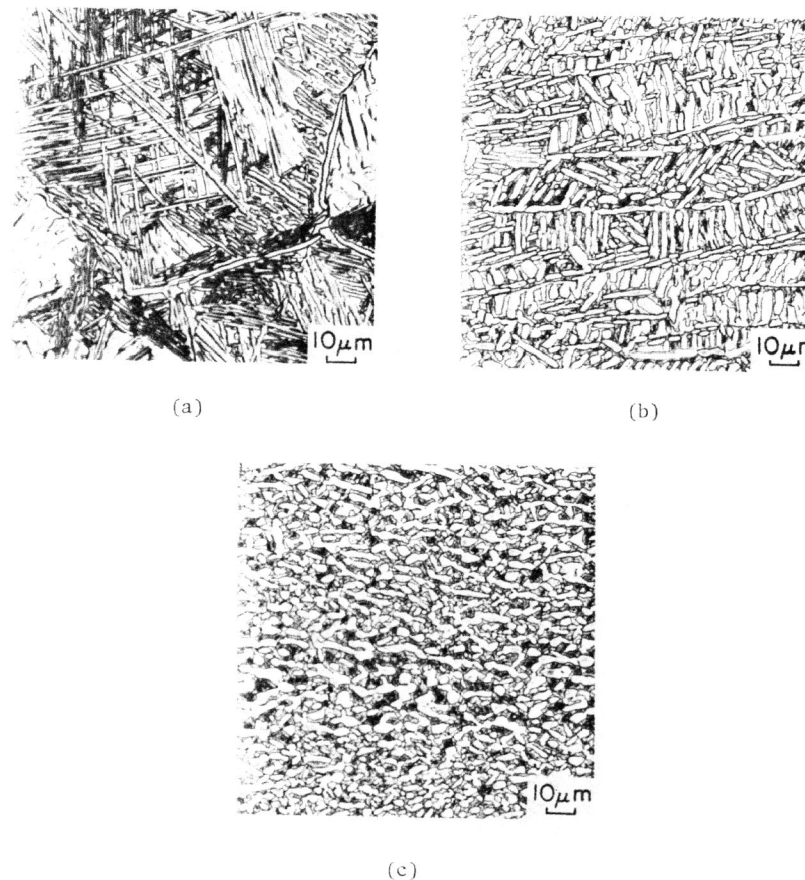
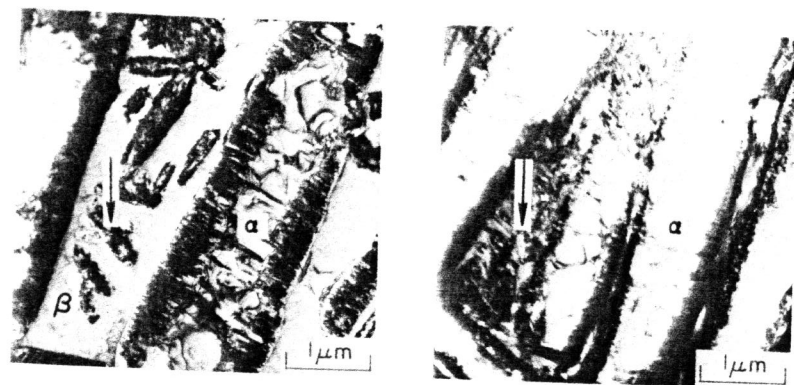


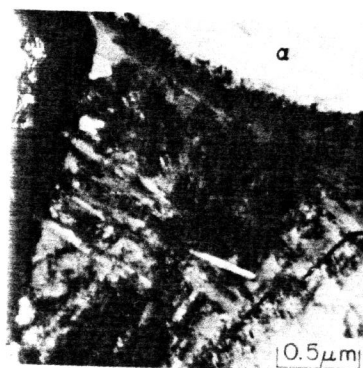
Figure 1 Light Micrographs Illustrating the Effect of Forging on Microstructure:

- (a) β -Forged
- (b) High α/β -Forged
- (c) Low α/β -Forged



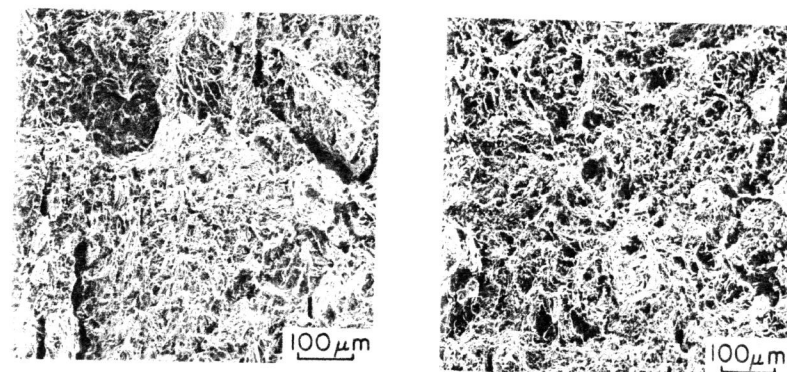
(a)

(b)



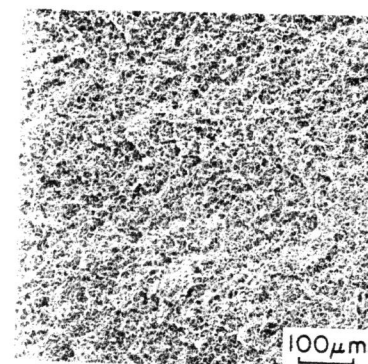
(c)

Figure 2 Transmission Electron Micrographs Illustrating the Effect of Final Heat Treatment on β -Forged Material:
 (a) Coarse α -Phase Particles Precipitated During High Final Treatment
 (b) and (c) Fine α -Phase Particles Precipitated During Low Final Treatment



(a)

(b)



(c)

Figure 3 Scanning Electron Fractographs of:
 (a) TL Specimen from β -Forged Material
 (b) TL Specimen from High α/β -Forged Material
 (c) TL Specimen from Low α/β -Forged Material